On quantifying the climate of the nonautonomous Lorenz-63 model

J. D. Daron and D. A. Stainforth

Articles you may be interested in

Configuration Management for Large-Scale Scientific Computing at the UK Met Office
Comput. Sci. Eng. **10**, 56 (2008); 10.1109/MCSE.2008.144

Global Weather Prediction and High-End Computing at NASA
Comput. Sci. Eng. **6**, 29 (2004); 10.1109/MCISE.2004.1255818

The Architecture of the Earth System Modeling Framework
Comput. Sci. Eng. **6**, 18 (2004); 10.1109/MCISE.2004.1255817

Testing and Evaluating Atmospheric Climate Models
Comput. Sci. Eng. **4**, 64 (2002); 10.1109/MCISE.2002.1032431

Distributed Computing for Public-Interest Climate Modeling Research
Comput. Sci. Eng. **4**, 82 (2002); 10.1109/5992.998644

On quantifying the climate of the nonautonomous Lorenz-63 model

J. D. Daron[1,a),b)] and D. A. Stainforth[2,c)]
[1]Climate System Analysis Group, University of Cape Town, Cape Town, South Africa
[2]Grantham Research Institute for Climate Change and the Environment, and Centre for the Analysis of Time Series, London School of Economics, London, United Kingdom

The Lorenz-63 model has been frequently used to inform our understanding of the Earth's climate and provide insight for numerical weather and climate prediction. Most studies have focused on the autonomous (time invariant) model behaviour in which the model's parameters are constants. Here, we investigate the properties of the model under time-varying parameters, providing a closer parallel to the challenges of climate prediction, in which climate forcing varies with time. Initial condition (IC) ensembles are used to construct frequency distributions of model variables, and we interpret these distributions as the time-dependent climate of the model. Results are presented that demonstrate the impact of ICs on the transient behaviour of the model climate. The location in state space from which an IC ensemble is initiated is shown to significantly impact the time it takes for ensembles to converge. The implication for climate prediction is that the climate may—in parallel with weather forecasting—have states from which its future behaviour is more, or less, predictable in distribution. Evidence of resonant behaviour and path dependence is found in model distributions under time varying parameters, demonstrating that prediction in nonautonomous nonlinear systems can be sensitive to the details of time-dependent forcing/parameter variations. Single model realisations are shown to be unable to reliably represent the model's climate; a result which has implications for how real-world climatic timeseries from observation are interpreted. The results have significant implications for the design and interpretation of Global Climate Model experiments. © 2015 AIP Publishing LLC.
[http://dx.doi.org/10.1063/1.4916789]

Over the past 50 years, insight from research exploring the behaviour of simple nonlinear systems has been fundamental in developing approaches to weather and climate prediction. The analysis herein utilises the much studied Lorenz-63 model to understand the potential behaviour of nonlinear systems, such as the climate, when subject to time-varying external forcing, such as variations in atmospheric greenhouse gases or solar output. Our primary aim is to provide insight which can guide new approaches to climate model experimental design and thereby to better address the uncertainties associated with climate change prediction. We use ensembles of simulations to generate distributions which we refer to as the "climate" of the time-variant Lorenz-63 model. In these ensemble experiments, a model parameter is varied in a number of ways which can be seen as paralleling both idealised and realistic variations in external forcing of the real climate system. Our results demonstrate that predictability of climate distributions under time varying forcing can be highly sensitive to the specification of initial states in ensemble simulations. This is a result which at a superficial level is similar to the well-known initial condition sensitivity in weather forecasting, but with different origins and different implications for ensemble design. We also demonstrate the existence of resonant behaviour and a dependence on the details of the "forcing" trajectory, thereby highlighting further aspects of nonlinear system behaviour with important implications for climate prediction. Taken together, our results imply that current approaches to climate modeling may be at risk of under-sampling key uncertainties likely to be significant in predicting future climate.

I. INTRODUCTION

Five decades after Edward Lorenz first encountered chaos in a low-dimensional model simulating thermal convection,[1] the study of chaotic behaviour in nonlinear systems remains highly relevant across a broad range of scientific disciplines. Aspects of the climate system are "unquestionably chaotic."[2] The consequences of this for weather forecasting are felt in the impact of initial condition (IC) uncertainty on the particular climatic state at some point in the future. The consequences for climate forecasting are evident in the combined impact of IC uncertainty and forcing variations on the future probability distributions of climatic variables; i.e., on future climate as a distribution.[3–5] If there are no forcing variations, then—as one moves from weather forecasting to seasonal, decadal and multi-decadal climate forecasting—these probability distributions approach those representative of the stationary climate attractor (if such a thing exists);

a)Electronic mail: jdaron@csag.uct.ac.za
b)Also at UK Met Office, Exeter, United Kingdom.
c)Also at Department of Physics, University of Warwick, Coventry, United Kingdom and Environmental Change Institute, University of Oxford, Oxford, United Kingdom.

uncertainty in a weather forecast becomes the distribution representative of the stationary system's variables. IC ensembles (ICEs) provide a means of studying the process of "climate prediction" with and without forcing variations, and are valuable for exploring the transient behaviour of nonautonomous nonlinear systems in general.

The work presented here aims to inform our understanding of the implications of IC uncertainties for climate forecasting; uncertainties that are poorly addressed in most climate modelling experiments. Results are discussed in relation to the real-world climate system, and models thereof, to demonstrate the relevance of these issues for climate prediction under transient forcings. They also have implications for how we characterise the transient behaviour of both nonlinear geophysical systems more generally, and nonautonomous nonlinear mathematical systems. We explore the role of macro-initial condition (macro-IC) uncertainty, which is described as uncertainty in "state variables with relatively large slowly mixing scales,"[6] to provide insight into the design of climate modeling experiments. Our findings imply not only a need for much larger IC ensembles than is common practice today but also that experimental designs should allow for the likelihood that model based probabilistic predictions will be macro-IC dependent. The results demonstrate that under transient changes in forcing, the concept of a changing climatic attractor is unhelpful because the transient distributions at a particular forcing value can be very different to the distributions representative of the attractor at the same, but unchanging, forcing value.

While the nonlinear systems community typically focus on the properties of *autonomous* dynamical systems—whose equations have no explicit dependence on time,[7] increasingly, and particularly in relation to climate research—attention is being given to nonautonomous dynamical systems whose equations are time-dependent.[3,8,9] Changes in the external forcings on the climate system (e.g., variability in the solar constant or changes in albedo or atmospheric greenhouse gas concentrations) are inherently time-dependent; the climate system itself is a nonautonomous dynamical system. We therefore focus on the behaviour of the nonautonomous L63 model which is achieved by varying the model's parameters and demonstrating numerically how this impacts its "climate."

Before detailing the methodology and experiments conducted, it is useful first to introduce two relevant concepts: resonance and the kairodic assumption.

Resonance is observed in a wide range of dynamical systems. It is most commonly used to describe a situation where a dynamical system oscillates with a greater amplitude when subject to forcing at specific (resonant) frequencies, but its interpretation for nonlinear systems can be more complicated.[10,11] The term *stochastic* resonance has been applied to those systems that display resonant behaviour as a function of the noise level in a system's parameter.[12] In the L63 model, resonant behaviour has been demonstrated[13–15] and some studies exploring stochastic resonance in this model have related their results to forcing variations on the climate system.[16,17] More recently, through studying stochastic resonance, Benzi (2010)[18] has

stressed that fast variables should not be ignored in the study of long-term climate change. None of these studies, however, have explicitly acknowledged the effects of resonance on ensemble distributions, which is critical for understanding transient climate change and thereby informing climate change adaptation decisions.[6] Herein, we will refer to distributions of model variables from ICEs as the model's climate,[3] which is, of course, conditioned on the particular design of the ICE, as will be illustrated

Though rarely acknowledged, the ergodic assumption is often applied in climate modeling.[19] Sprott (2003)[20] states: "the ergodic hypothesis[21] asserts that the probability distribution is the same for many iterations of a single orbit (time average) and for a high-order iteration of many orbits with a range of random ICs (ensemble average)." The concept described is useful in model interpretation, although more usually a system can only be deemed ergodic when considering its infinite time properties.[22,23] To allow for the analysis of dynamical sytems over finite periods, in this paper we utilise and test the related "kairodic assumption" introduced by Daron and Stainforth (2013)[3] in which "the distribution over time is [taken as] representative of the distribution of possible states at an instant." This encapsulates both the concept described by Sprott (2003)[20] when considering "high order iterations" and "many orbits," as well as common practice in climate science where observational or model distributions over a fixed period of time, often 30 years,[24–26] are taken to represent the system's climate within that period.

We begin, in Sec. II, by presenting the L63 model's climate distributions under fixed parameters using both a single trajectory and IC ensembles. After an initial qualitative analysis, the impact of simulation length on the two approaches is quantified using the Jensen-Shannon divergence (JSD).[27] The impact of macro-IC uncertainty is addressed in Sec. III by investigating the rates of convergence for model ensembles originating in different regions of the model's state space. In Sec. IV, the behaviour of the model with various values of the parameter ρ is presented. This provides the context for Secs. V and VI, which show results from experiments with periodic and nonperiodic fluctuations in ρ, respectively. Finally, Sec. VII discusses the implications of our results for climate model experimental design and the interpretation of climate model output.

II. THE L63 CLIMATE

A. L63 model

The L63 model consists of three ordinary differential equations which describe thermal convection in a fluid:

$$\frac{dX}{dt} = \sigma(Y - X), \tag{1}$$

$$\frac{dY}{dt} = X(\rho - Z) - Y, \tag{2}$$

$$\frac{dZ}{dt} = XY - \beta Z. \tag{3}$$

X, Y, and Z are the model variables, σ is the Prandtl number, ρ is the Rayleigh number, and β is a geometric factor.[1,28] We begin by considering parameters with values: $\sigma = 10$, $\rho = 28$, and $\beta = \frac{8}{3}$, as in Lorenz (1963).[1] Model simulations are performed using a fourth-order Runge-Kutta integration scheme with a time step, $\tau = 0.001$ Lorenz Time Units (LTUs).

The L63 model evolves with two characteristic time scales: an oscillation time around a regime centroid and a residence time within a regime.[29] An oscillation typically occurs on a time scale of ~ 1 LTU while the residence time, the time between regime transitions, varies and is subject to chaos such that the distance in state space between trajectories with similar ICs initially diverges on average exponentially with time;[1,30] eventually, the growth rate decreases until the size of the average separation is equal to the distance between two randomly selected states. Uncertainty in the initial state limits deterministic predictability, but one can estimate the model variable probability distributions at any point in the future using an IC ensemble conditioned on IC uncertainty. In relating this work to models of climate, such IC uncertainty can be considered as representing observational uncertainty when initialising a perfect model of a real-world system.

Two methods are available for numerically estimating the distributions of the L63 variables on the model's attractor (in our terminology these distributions are the stationary climate of the model for each variable). The first option uses a single realisation of the model run for a long period of time (relative to the dynamic time scales of the model) to generate a frequency distribution for each model variable. In the second, a large IC ensemble is run for a fixed length of time, and the final states of each member are used to generate the frequency distributions. To inform the design of modelling experiments in climate-like problems, an important question is whether these two methods produce the same results (i.e., is the kairodic assumption[3] valid for fixed parameter values and if so on what timescales). Our starting point is therefore to make this assessment.

B. Convergence of single trajectory distributions

Fig. 1 shows the frequency distributions for Z from a single model realisation but generated from increasing length simulation periods—1 LTU to 10 000 LTUs; the corresponding distributions for the Y and Z variables are given in the supplementary material (Ref. 31, Figs. S1 and S2). The single model trajectory was initiated from a point close to (but not on) the attractor: the chosen IC is $(X, Y, Z) = (1.0, 1.0, 25.0)$, a state near the saddle point of the attractor.

Fig. 1(a) shows the distribution of model states over the first LTU of the model simulation. The distribution is highly asymmetric, but as longer periods are considered in the construction of the distributions this asymmetry decreases and the distributions become more similar. The distribution after 10 000 LTUs (Fig. 1(i)) is relatively smooth with a primary peak at $Z \approx 18$ and a secondary peak at $Z \approx 34$. The distributions in X and Y show convergence on similar timescales (Ref. 31, Figs. S1 and S2).

C. Convergence of initial condition ensemble distributions

To generate IC ensemble distributions, we take a 100 000 member ICE with ICs spaced evenly along a one-dimensional transect[2] X_l, Y_l, $Z_l = (-20, -25, 1)$ to X_h, Y_h, $Z_h = (20, 25, 40)$ through the region of model state space occupied by the attractor. The ensemble is run for 1000 LTUs. The distribution of Z across the ensemble at specific time instants in the simulation period are shown in Fig. 2; corresponding distributions for X and Y are provided in the supplementary material (Ref. 31, Figs. S3 and S4). Fig. 1(i) closely resembles the ensemble distribution shown in Fig. 2(i) suggesting that the use of the kairodic assumption is valid in the L63 model with fixed parameters; for the values used here. The distributions are, however, clearly different.

One reason is the size of the ensemble. While a 100 000 member IC ensemble would be considered very large in a climate modelling context, the number of individual data points is two orders of magnitude smaller than the 10 million data points that constitute the distribution given in Fig. 1(i). It might also be that a 1000 LTU integration period is still too short for the ensemble members to represent IC-independent samples of the attractor. Whether or not this is the case is addressed in Sec. II D.

D. Convergence towards the model climate

To facilitate the evaluation of the difference between the distributions using the two methods, and the rate at which each method converges to a stationary climate, we take the 100 000 member IC distributions after 1000 LTUs as "standard" distributions representative of the L63 model's stationary climate. For reference, Fig. 3 shows these distributions; Fig. 3(c) is a reproduction of Fig. 2(i). The ensemble distribution is used for this purpose for consistency with later analysis under time varying parameters where the single trajectory distribution would not be a relevant option.

The simulation time for frequency distributions extracted from a single trajectory to approach the standard distributions might be expected to be longer than that for an IC ensemble because a single trajectory can remain in one regime for a long time but it is less likely that a large fraction of an ensemble will do the same. This is indeed the case, as is evident by comparing Fig. 1(e) to Fig. 2(g). Both show frequency distributions after a 100 LTU and have the same number of constituent data points, but the distribution from the single trajectory (Fig. 1(e)) is clearly different from the standard stationary climate distribution (Fig. 3(c)) while the ensemble distribution (Fig. 2(g)) is more similar.

To make quantitative comparisons between these distributions, we use the Jensen-Shannon Divergence (JSD);[27] a variation on relative entropy, also known as the Kullback-Leibler divergence.[32] Like relative entropy, the JSD provides a measure of similarity between two probability distributions. Unlike relative entropy, the JSD always produces a finite value making it preferable in this study where the distributions we compare are sometimes non-overlapping. For two discrete probability distributions Q and P, the JSD is given by
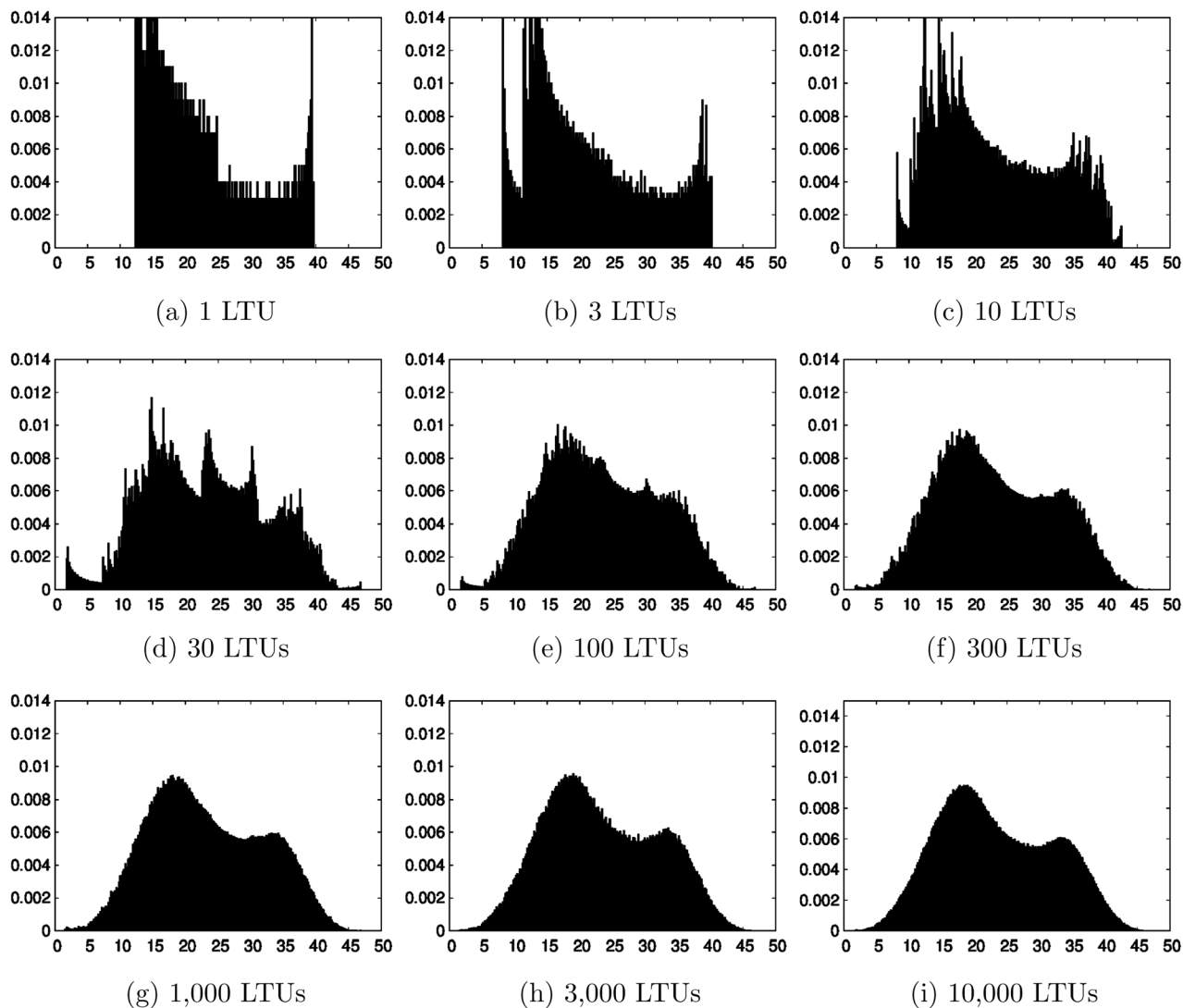
FIG. 1. Normalised frequency distributions of the Z variable from a single trajectory of the L63 model over increasing time periods; ICs $(X, Y, Z) = (1.0, 1.0, 25.0)$. The x-axis corresponds to the Z variable, and the y-axis corresponds to the frequency of states per bin; bin width $= 0.2$. Some density in panels (a)–(c) extends beyond the scale.

equations (4) to (7) in which Eq. (5) and Eq. (6) define the relative entropy, D, between distributions P and M, and Q and M, respectively.

$$JSD(P \parallel Q) = \frac{1}{2}D(P \parallel M) + \frac{1}{2}D(Q \parallel M), \qquad (4)$$

$$D(P \parallel M) = \sum_i \ln\left(\frac{P(i)}{M(i)}\right)P(i), \qquad (5)$$

$$D(Q \parallel M) = \sum_i \ln\left(\frac{Q(i)}{M(i)}\right)Q(i), \qquad (6)$$

$$M = \frac{1}{2}(P + Q). \qquad (7)$$

The JSD between two 10 000 member random samples of the standard stationary climate distributions is calculated and the process repeated 1000 times to produce a distribution of JSD values (see Table I). The samples are taken from the same population so the JSD values reflect differences resulting only from the size of the samples. This provides indicative values to help in the interpretation of model distribution comparisons. When comparing different evaluations of the standard stationary climate distributions, a JSD value below two standard deviations greater than the mean (i.e., $\text{JSD}(X) < 1.78 \times 10^{-3}$, $\text{JSD}(Y) < 2.33 \times 10^{-3}$, and $\text{JSD}(Z) < 2.09 \times 10^{-3}$) indicates that the underlying distributions cannot be identified as different at above the 97% confidence level. If the distributions cannot be confidently identified as different, then we consider them to be indistinguishable and describe them as having converged. Similarly, if they can be confidently identified as different, then they are considered to be distinguishable and not to have converged.

In Fig. 4, the standard stationary climate distributions (Fig. 3) are compared to the distributions resulting from both the single trajectory method and the IC ensemble method. As expected, the ensemble distributions converge more rapidly than the single trajectory distributions towards the standard stationary climate distribtutions. After 50 LTUs, the
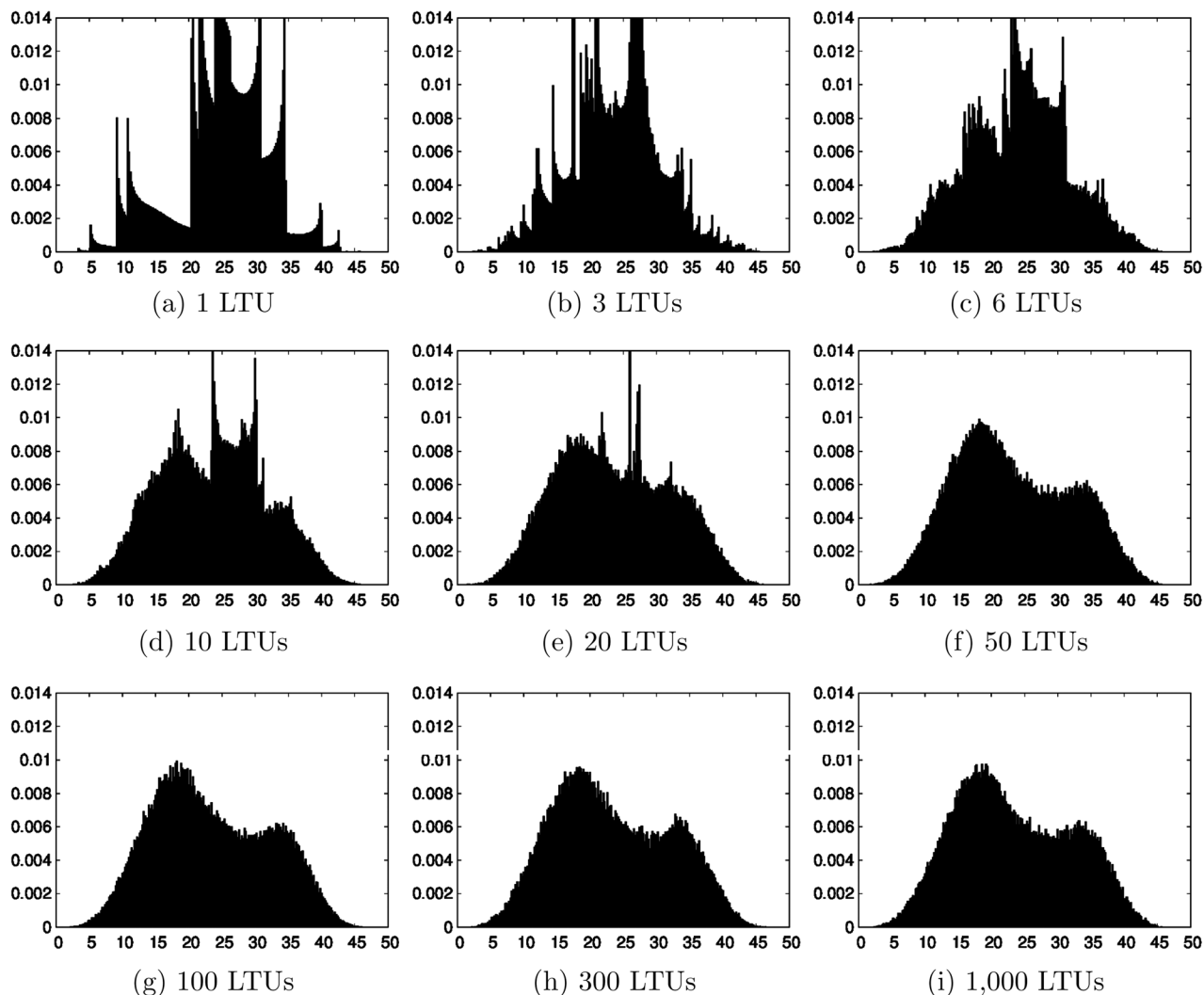
FIG. 2. Normalised frequency distributions of the Z variable from a 100 000 member IC ensemble with ICs spread evenly along a transect, from (X_l, Y_l, Z_l) $= (-20, -25, 1)$ to $(X_h, Y_h, Z_h) = (20, 25, 40)$. Distributions show the states of each ensemble member at a given time instant in the simulation period. The x-axis corresponds to the Z variable, and the y-axis corresponds to the frequency of ensemble members per bin; bin width $= 0.2$. Some density in panels (a)–(c) extends beyond the scale.
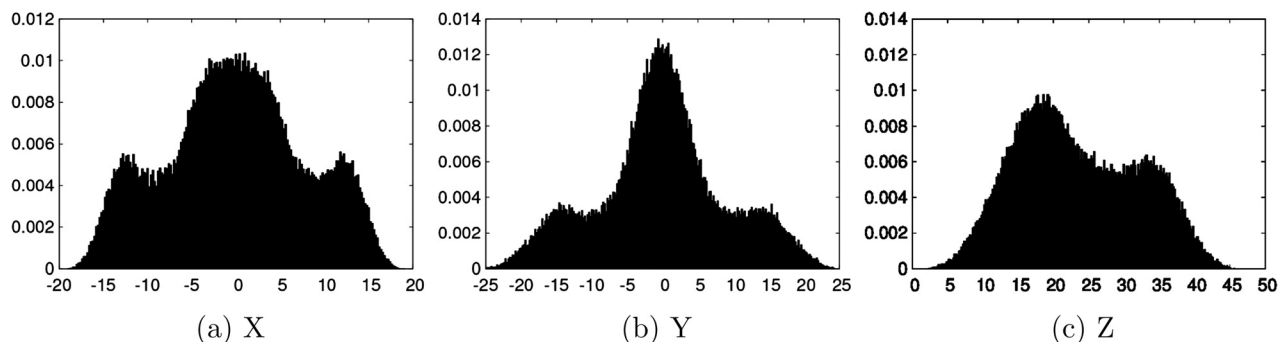

FIG. 3. Normalised frequency distributions for the L63 model variables, from a 100 000 member IC ensemble with ICs spread evenly along a transect: $(X_l, Y_l, Z_l) = (-20, -25, 1)$ to $(X_h, Y_h, Z_h) = (20, 25, 40)$. The distributions show the states of each ensemble member at 1000 LTUs in the simulation period. The x-axis is given in each panel title, and y-axis as in Fig. 2. These distributions are referred to throughout as the "standard" distributions representative of the L63 model's stationary climate.

ensemble distributions have converged while the single trajectory method requires an additional 350 LTUs before the same can be said of them. The single trajectory convergence is also less smooth, presumably due to long residence times within the regimes of the attractor.

III. MACRO-INITIAL CONDITION MEMORY IN THE L63 MODEL

Having demonstrated that the kairodic assumption is valid for a sufficiently large number of iterations (that an IC ensemble and a single trajectory converge towards the same

TABLE I. Statistics of JSD values ($\times 10^{-3}$) for Lorenz-63 values taken from 1000 comparisons of two randomly drawn 10 000 member samples from the standard climate distributions.

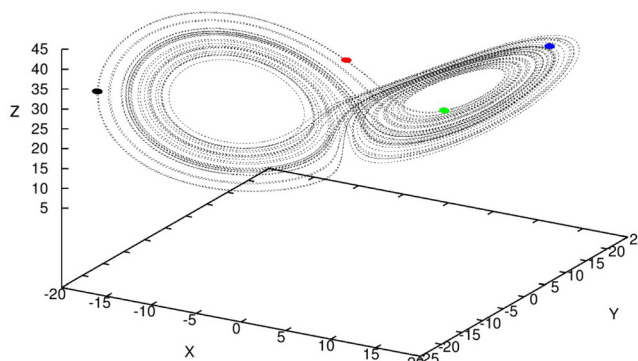| JSD statistic	$X (\times 10^{-3})$	$Y (\times 10^{-3})$	$Z (\times 10^{-3})$
Minium	0.66	0.73	0.78
Mean	1.24	1.59	1.49
Maximum	2.49	2.88	2.87
Standard deviation	0.27	0.32	0.30

FIG. 5. Single trajectory for a 50 LTU simulation of the L63 model with ICs $(X, Y, Z) = (1.0, 1.0, 25.0)$ (dashed line), and the starting locations for four 10 000 member IC ensembles (coloured dots). Members of the ensembles are generated by addition of a perturbation from a central value in all dimensions X, Y, and Z. The perturbations are samples from a Gaussian distribution with standard deviation 0.2. The central values for the IC ensembles are (from left to right): **1**—black cluster $(-17.228, -22.383, 34.031)$; **2**—red cluster $(-2.520, 5.867, 31.340)$; **3**—green cluster $(6.683, 9.593, 20.451)$; and **4**—blue cluster $(15.668, 15.564, 36.882)$.

standard stationary climate), we address the question of whether the choice of ICs affects the rate of convergence.

For climate and environmental prediction, if we had a perfect model of our system, then we would want to initiate ensembles from states consistent with observations of reality. Indeed, this is already done with today's models; a subset of the CMIP5[33] GCM experiments was initiated with ICs which reflect observations of the recent climatic state, specifically in respect of the oceans. Yet, even with the best conceivable observing system, the exact initial state is of course subject to uncertainty, but an ICE can be constructed in which the ICs reflect the remaining uncertainty at the smallest scales (micro-IC uncertainty[6]). Large scale differences in the state of the system (e.g., states of the thermohaline circulation, El Nino Southern Oscillation, or stratospheric circulation patterns) represent substantially different initial states (macro-IC[6]); some may retain information and therefore a degree of predictability for longer than others. These states may or may not be distinguishable with current observing systems but are in principle distinguishable with potentially achievable observing systems.

To explore the impact of macro-IC uncertainty in the L63 model, 10 000 member IC ensembles are initiated from four different non-overlapping regions of model state space, illustrated in Fig. 5. The time it takes for the different ICEs to converge provides a measure of the *memory in distribution* of the macro-ICs and demonstrates the impact of IC ensemble location on climate predictability within the model. We use the term memory to refer to the length of time for which a distribution remains distinguishable (see Sec. II D) from the standard stationary climate distribution. When the ensemble distributions have converged to the standard stationary climate distributions (see Fig. 3), the memory of IC ensemble location has been lost. This approach builds on

earlier studies related to short- and medium-term weather prediction[29,34,35] by providing a climate distribution perspective to "limits of predictability." In doing so, it facilitates its further development to nonautonomous systems in Secs. V and VI.

Fig. 6 shows that each of the four IC ensembles converge towards the standard stationary climate distributions, with memory of the macro-ICs lost on a timescale of 30–40 LTUs. This is slightly faster than in the ICE of Sec. II A (see Fig. 4) because the former ensemble assumed little knowledge of the attractor so many members were initiated far from it; the parallel in climate modelling would be to initiate a model with little knowledge of what states would be physically consistent with the model. After 5 LTUs there remain large differences between the four ensemble distributions; the JSD values range from $JSD \approx 0.14$ (IC 2 in Z) to $JSD \approx 0.44$ (IC 2 in X). This indicates memory of the macro-ICs and therefore a degree of predictability. Even after 20 LTUs, there remain distinguishable differences from the standard stationary climate. Furthermore, some IC ensembles converge faster than others for some variables— IC4 converges towards the standard stationary climate faster than the other ensembles for the X and Y variables. This is
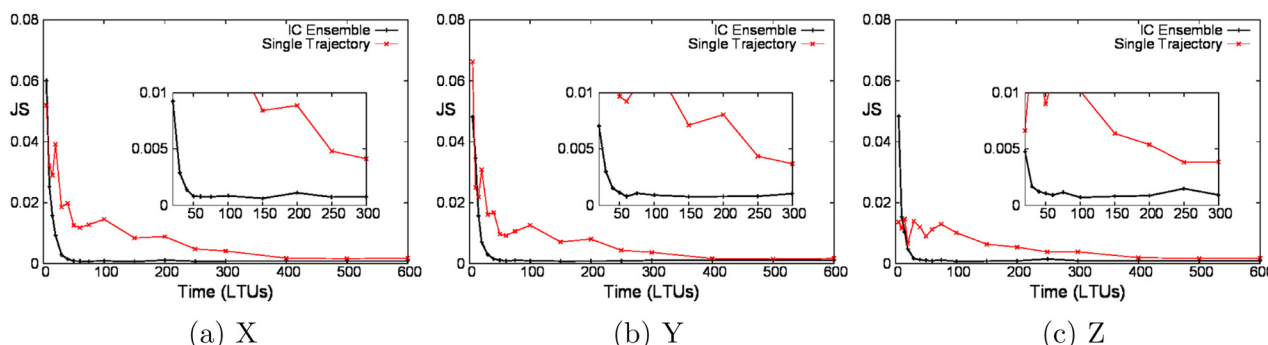

(a) X

(b) Y

(c) Z

FIG. 4. JSD results showing the comparisons between the standard climate distributions and the distributions from single trajectory distributions and IC ensembles for each of the L63 model variables under fixed (conventional) parameter conditions.
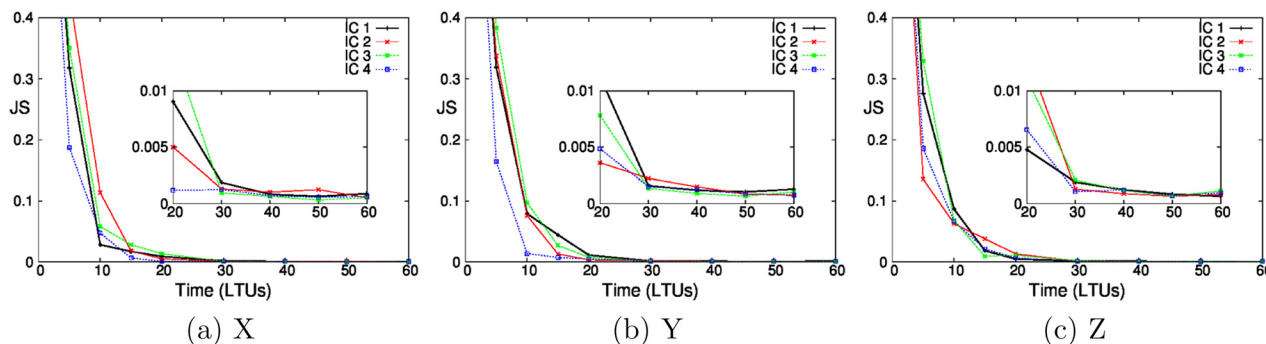
FIG. 6. JSD results showing the comparisons between IC ensemble distributions from IC locations shown in Fig. 5, to the distributions resulting from an IC ensemble with ICs taken from the standard distributions, at given time intervals for fixed parameter values.

likely because the initial location of the IC4 ensemble means that trajectories approach the saddle point of the attractor more quickly than those initiating from the other ensembles, allowing the ensemble to spread across the attractor state space more quickly.

IV. VARYING THE PARAMETER ρ

So far the focus has been on the role of ICs in climate prediction in a stationary system. The most valuable lessons from L63 for climate prediction, however, may come from its behaviour with time-dependent parameters; a nonautonomous system. Introducing a time-dependence to one of the L63 model parameters can be considered a parallel to variations in forcings on the real world climate system such as that resulting from changes in solar energy input or changing concentrations of atmospheric greenhouse gas concentrations. It also provides insight into the behaviour of a nonlinear dynamical system when subject to varying forcings. Before taking that step, however, it is useful to consider how the attractor and the stationary climate of the system, varies as parameters change.

The L63 model is a simplification of Rayleigh-Bernard thermal fluid convection between two vertically displaced plates of unequal temperatures. An increase in the temperature difference between the plates (represented by ρ) leads to an increase in the heat flux (denoted by Z). The impact of altering ρ has been likened to the impact of changes in the meridional temperature gradient on the equator to pole heat flux.[35] We therefore choose to focus on ρ when exploring parametric variations.

In the L63 system when $\rho < 1$, all trajectories propagate towards the origin (0, 0, 0), which is globally attracting.[36] For $\rho \geq 1$, the origin becomes unstable and two new stable fixed points emerge at coordinates $C^{\pm} = (\pm\sqrt{\beta(\rho-1)}, \pm\sqrt{\beta(\rho-1)}, \rho-1)$. At the value $\rho = 24.74$ (ρ_H), a Hopf bifurcation occurs. For values of $\rho > \rho_H$, the fixed points located at $C^{\pm}$ become unstable and the system becomes chaotic.[37] Since chaos is considered an inherent part of the climate system,[2] we choose to focus on the climate of the L63 model when $\rho > \rho_H$.

Figure 7 shows frequency distributions of the Z variable for different fixed values of ρ, determined from 10 000 member IC ensembles after a simulation period of 100 LTUs. As

ρ increases from $\rho = 25$ to $\rho = 31$, there is a shift in the distribution towards higher values of Z; the maximum value of Z increases from $Z_{max} = 41.0$ to $Z_{max} = 50.9$, the mean value increases from $\bar{Z} = 20.5$ to $\bar{Z} = 26.4$ while the minimum value shows relatively little change, moving from $Z_{min} = 2.5$ to $Z_{min} = 3.4$. As the parameter ρ increases, the range in Z increases and the peaks become less pronounced (whilst shifting to higher values), but the general shape of the distribution is preserved. With this information as context, we now proceed to investigate the behaviour of the L63 model under fluctuating parameter conditions.

V. PERIODIC OSCILLATIONS IN ρ

A. Impact of periodic forcing variations on the L63 model climate

First, we present the behaviour of the L63 model when subject to smoothly varying periodic fluctuations in ρ; in Sec. VI, nonperiodic variations are addressed. Perturbations are added to a reference value, ρ_0, in the form of a sinusoidal time series:

$$\rho(t) = \rho_0 + A(\sin 2\pi ft), \tag{8}$$

where A is the wave amplitude, t represents time (units LTU), and f is the frequency of the wave (units LTU^{-1}).

A range of frequencies ($0.1 \leq f \leq 10$) are investigated, and ρ_0 is fixed at $\rho_0 = 28$ with $A = 3$ so that ρ oscillates between 25 and 31; the range presented in Sec. IV. For each value of f, a 10 000 member IC ensemble is run using initial values sampled from across the stationary, $\rho_0 = 28$ attractor (the states are taken from those used in the construction of the standard stationary climate distributions—Fig. 3). Fig. 8 shows the impact of periodic variations in ρ on the distributions after 40 LTU. For all frequencies studied, $\rho = 28$ after 40 LTU.

When $f = 0$, the ensemble distribution (Fig. 8(a)) is, by design, similar to the standard stationary climate distribution shown in Fig. 3(c) (note different y-axis scale), albeit less smooth because of the smaller number of ensemble members. For a low frequency oscillation, $f = 0.1$, the distribution (Fig. 8(b)) is not substantially altered. For relatively high frequency oscillations (e.g., when $f = 10$) the distribution (Fig. 8(f)) is also similar to the standard climate distribution. At such frequencies, the rapid perturbations to ρ have little
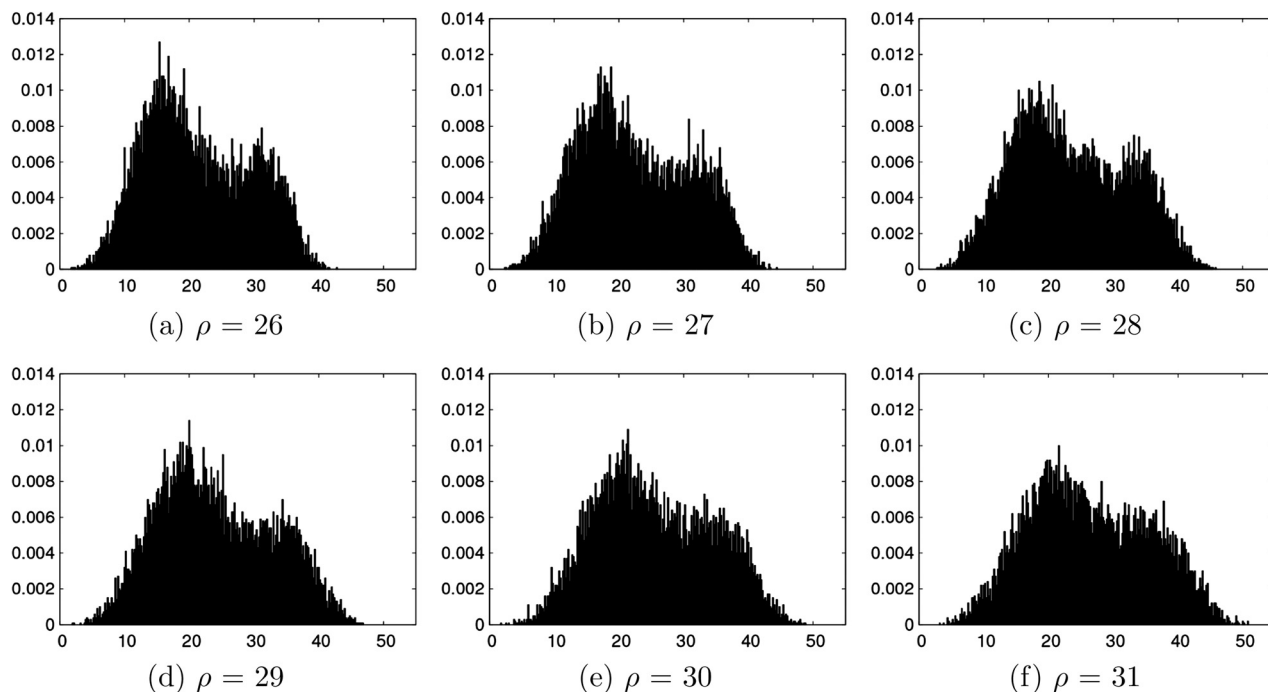
FIG. 7. Normalised frequency distributions for the Z variable from a 10 000 member IC ensemble after 100 LTUs, for different values of ρ. The IC ensembles are initiated with ICs taken from the first 10 000 members of the standard climate distributions for $\rho = 28$, shown in Fig. 3. The x-axis corresponds to the variable Z, and y-axis as in Fig. 2.

impact and the model behaves in a similar way to that observed for the fixed parameter $\rho_0 = 28$. When $f = 1$, $f = 3$, and to a lesser extent when $f = 5$, however, the distributions are substantially different to the standard stationary climate distributions. At $f = 1$, ρ oscillates on a similar time scale to the attractor regimes' orbiting frequency. The model appears to be resonating as a result of the fluctuations in ρ. This

resonance leads to dramatic changes in the distributions of the model variables, the model's climate.

How the distributions vary in time is shown in Fig. 9 in terms of their difference from the standard stationary climate distributions. The greatest differences are observed when $f = 1$, but they are also substantial when $f = 3$, particularly in the Z variable. For $f = 0.1$ and $f = 10$, the differences are
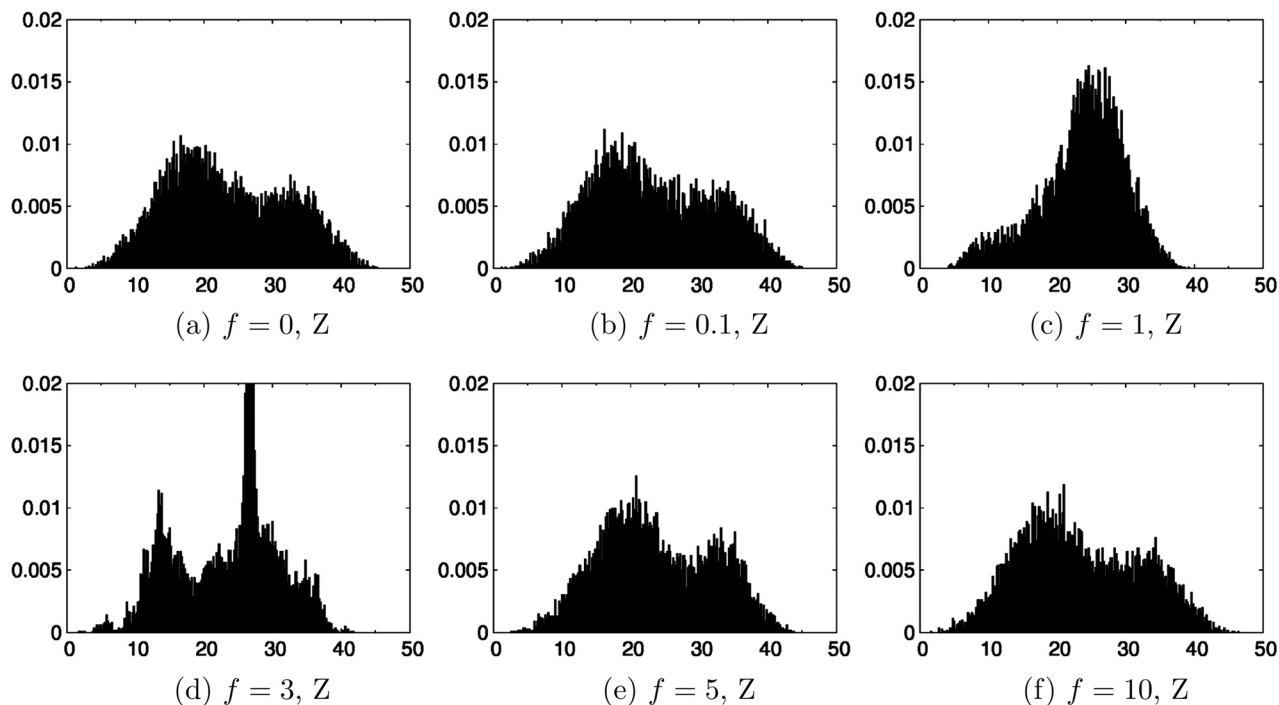

FIG. 8. Normalised frequency distributions of Z for a 10 000 member IC ensemble after a 40 LTU model run for given values of f. ICs extracted as in Fig. 7, and y-axis as in Fig. 2. Some density in panel (d) extends beyond the scale.
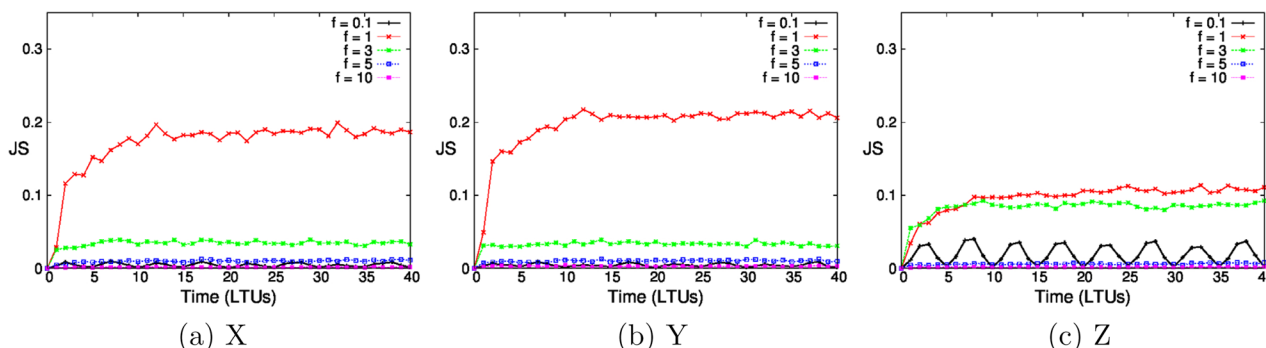
FIG. 9. JSD results showing comparisons between the ensemble distributions when $f = 0$ (i.e., ρ is fixed at $\rho = 28$) and the ensemble distributions for other values of f for each of the L63 model variables subject to periodic variations in ρ.

small except in the Z variable for $f = 0.1$. When $f = 0.1$, the distributions themselves oscillate, tracking the distributions representative of the fixed value of ρ at each point in time which returns to $\rho = 28$ every 5 LTU. This is most evident in the Z variable (Fig. 9(c)).

B. The kairodic assumption and periodic variations

In terms of methods to quantify the behaviour of nonlinear dynamical systems, it is relevant to ask whether the kairodic assumption holds under periodic fluctuations in ρ. That is to say, can the model's climate be quantified equally well by a long single realisation and a somewhat shorter IC ensemble? The answer is yes—for the parameter variations studied here, and with some conditions.

To reflect the climate of the oscillating system, we compare ensembles from a single trajectory with ensemble distributions constructed from an entire cycle in ρ rather than at a

specific instant in time. We focus on the $f = 1$ case in which the impact of the oscillations is greatest. Ensemble distributions are extracted from the last oscillation in ρ over the 40 LTU model simulations used to construct Fig. 8 (i.e., from 39 to 40 LTUs). Over one cycle at $f = 1$, the 10 000 member ensemble generates a distribution containing 10 million data points. To produce equivalent size distributions from a single trajectory, the model is run for 10 000 LTUs, and states are extracted at each time step. The resulting single trajectory and IC ensemble distributions are shown in Fig. 10. The two sets of distributions appear to be almost identical; the JSD values between them are <0.001. It is very unlikely that they could be confidently distinguished as samples from different underlying distributions. Thus, even with a sinusoidal time-varying parameter ρ, shown to induce resonant behaviour in the model, the kairodic assumption is still effective to estimate the model's climate distributions over one cycle for this model setup.
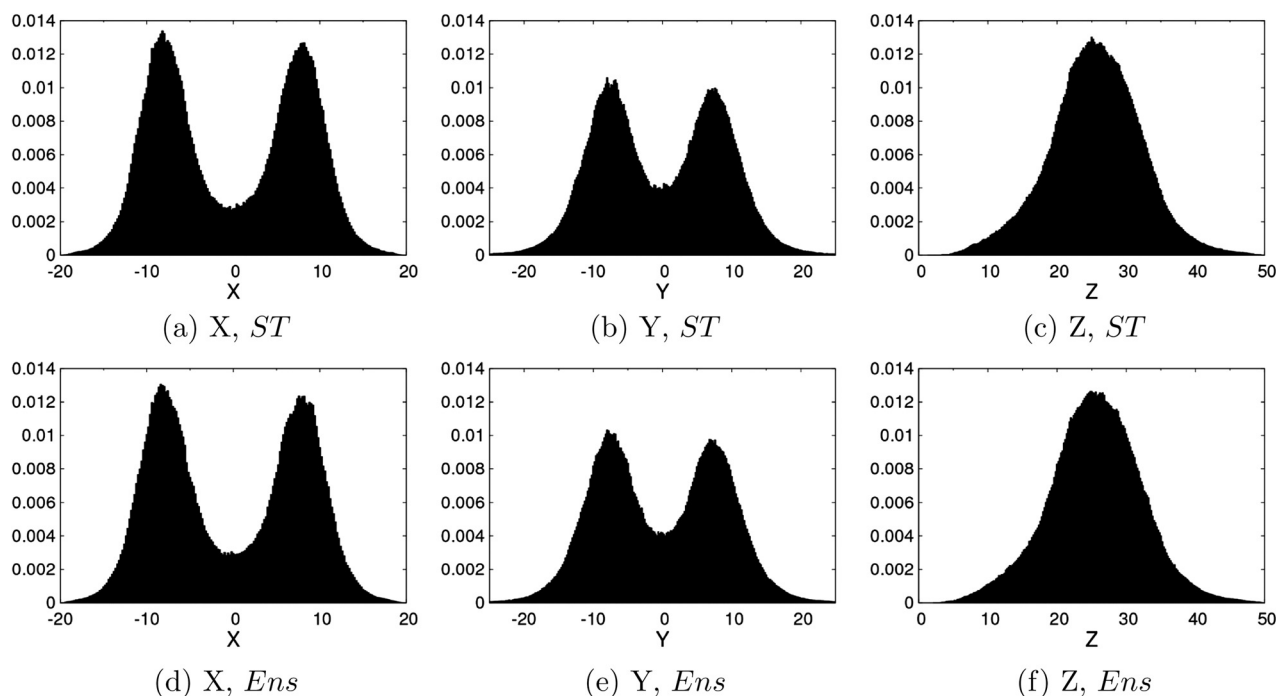

FIG. 10. Normalised frequency distributions for the L63 model when $f = 1$. Panels (a)–(c) correspond to single trajectory distributions (*ST*) for a 10 000 LTU model simulation and panels (d)–(f) correspond to IC ensemble distributions (*Ens*) extracted from all time steps in the last LTU of a 40 LTU model simulation (with ICs taken from the standard climate distributions). Y-axis as in Fig. 2.
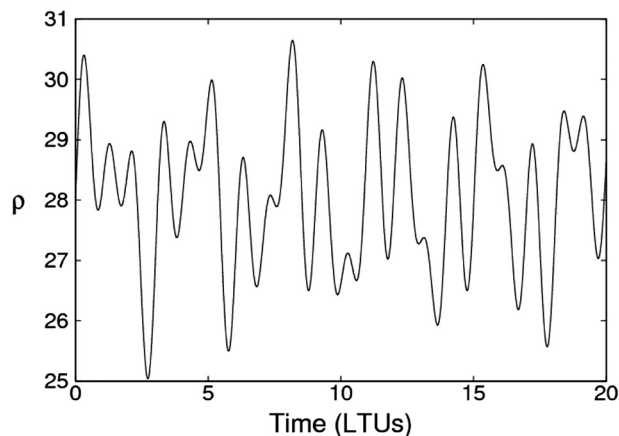
FIG. 11. Time series of fluctuations in ρ over 20 LTUs; $A = 3, f_i = 1$ according to Eq. (10).

It should be emphasised that the kairodic assumption is only effective here when the periodicity is appropriately accounted for. The difference between Fig. 8(c) and Fig. 10(f) demonstrates that the kairodic assumption fails when considering the distribution at a particular point in time, but the above analysis demonstrates that it can be applied when the ensemble distribution is calculated over a cycle. It is also expected to be appropriate if the single realisation was sampled only at the same point in the cycle as that used to construct an ensemble distribution.

VI. NONPERIODIC FLUCTUATIONS IN ρ

A. Introducing nonperiodicity

In reality, the climate system, and most environmental systems, is not subject to simple regular periodic forcing but

rather to a combination of forcings at different frequencies. How would such nonperiodic variations affect the climate of the L63 model? To study this, a nonperiodic time series in ρ is generated as follows:

$$\psi(t) = A\left(\frac{1}{3}\sin(2\pi f_i t) + \frac{1}{3}\sin\left(\sqrt{3}f_i t\right) + \frac{1}{3}\sin\left(\sqrt{17}f_i t\right)\right),$$
(9)

$$\rho(t) = \rho_0 + \psi(t),$$
(10)

where A is the wave amplitude, t represents time, and f_i is a parameter used to simultaneously adjust the frequencies of the three component waves (units LTU^{-1}). The three sine wave frequency multipliers are chosen as 2π, $\sqrt{3}$ and $\sqrt{17}$ so that the wave is both nonperiodic and non-repeating over *long* simulations. Fig. 11 shows the time series of ρ over 20 LTUs, when $A = 3$ and $f_i = 1$.

B. Impact of nonperiodic forcing variations on the L63 model climate

As in Sec. V 10 000 member IC ensembles are run for 40 LTUs, but this time with nonperiodic variations in ρ. When the fluctuations are slow or fast, the distributions for Z at 40 LTU (Figs. 12(a) and 12(f)) closely resemble the standard stationary climate distributions as they did in the periodic case. For intermediate frequencies of the parameter fluctuations, the distributions differ substantially from the standard stationary climate distributions (e.g., Fig. 12(c)). Because ρ varies nonperiodically, the value of ρ is different after 40 LTUs for each different value of f_i. One might therefore expect some differences between the distributions. As in the periodic case, however, the variation in the shape of the distributions is much greater than that seen in the distributions
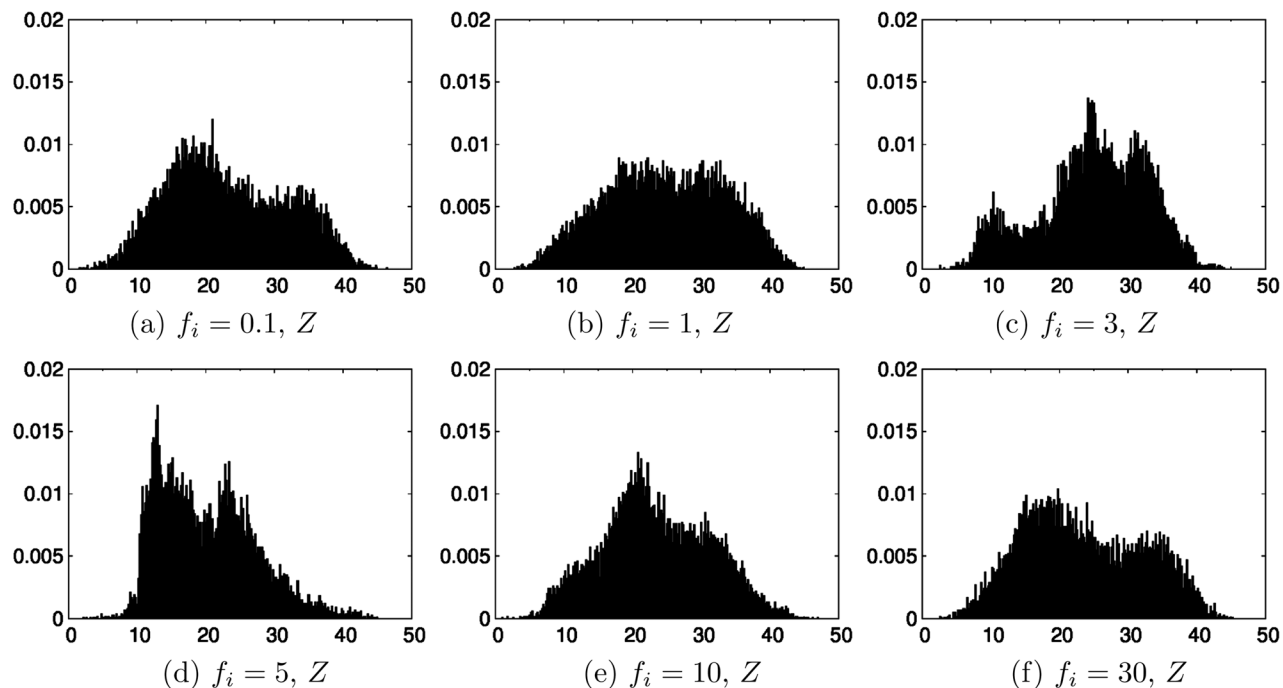

FIG. 12. Normalised frequency distributions of Z for a 10 000 member IC ensemble after a 40 LTU model run for given values of f_i. ICs are taken from the first 10 000 members of the standard climate distributions and y-axis as in Fig. 2.
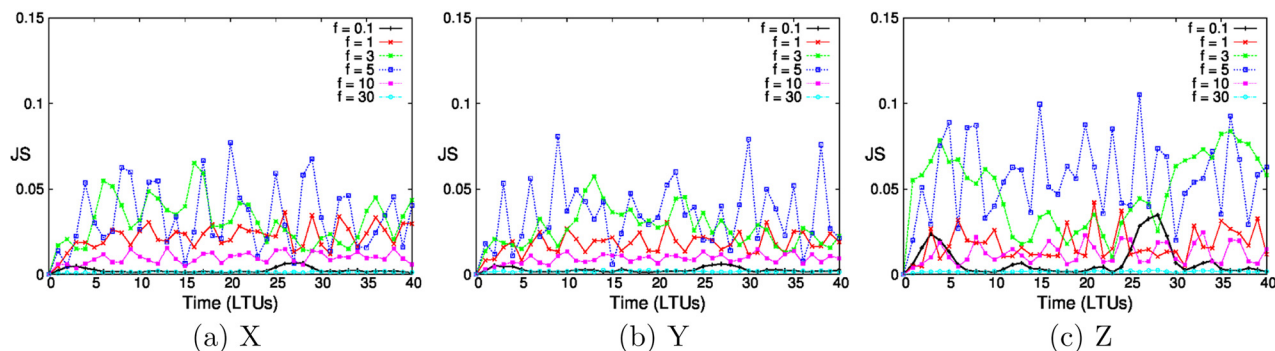
FIG. 13. JSD results showing comparisons between the ensemble distributions when $f_i = 0$ (such that ρ is fixed at $\rho = 28$) and the ensemble distributions for other values of f_i for each of the L63 model variables subject to nonperiodic variations in ρ.

representative of the fixed parameter attractors for ρ between $\rho = 25$ and $\rho = 31$ (Fig. 7).

The distributions vary greatly in time, as shown by the variability in the JSD comparison with the standard stationary climate distributions (Fig. 13). The largest differences occur at $f_i = 3$ and $f_i = 5$ when some of the frequencies of the nonperiodic forcing are close to the frequency of the orbit oscillations of the model trajectories; we therefore infer the likely presence of resonance. The JSD values are lower when $f_i = 1$ and $f_i = 10$, but there are, nevertheless, substantial differences in the distributions. The time series for Z when $f_i = 0.1$ (Fig. 13(c)) shows a similar effect to that seen in the periodic case where the distribution follows variations in ρ; the highest JSD values correspond to the peaks and troughs in ρ.

C. Path dependence in the L63 model with nonperiodic forcings

The above analysis demonstrates that resonance is an important factor in determining the climate distributions of the L63 model under periodic and nonperiodic variations in ρ. A further question is whether path dependence significantly influences the model's climate distributions—i.e., to

what extent do the ensemble distributions depend on the forcing history? To examine this question, model climate distributions are examined for two "forcing" time series' in ρ. One time series is the inverse of the other; the time series for ρ is inverted by multiplying $\psi(t)$ by -1. The model climate distributions are extracted at time instants when the fluctuating parameter ρ returns to the reference value $\rho = \rho_0 = 28$; this occurs, by design, at the same time in both time series. The corresponding IC ensemble distributions from the original and the inverted timeseries are shown in Fig. 14. They are substantially different. These differences imply that the L63 model climate is not only sensitive to the frequency of fluctuations in ρ but also to the specific time series in ρ; i.e., the "forcing" pathway.

D. Implications for the kairodic assumption

The path dependence of the IC ensemble distributions indicates that the kairodic assumption cannot be applied over long periods; the IC ensemble frequency distributions at an instant will be different from the frequency distributions over a *long* time interval of a single model trajectory, as was also the case under periodic variations at some frequencies. Could the kairodic assumption nevertheless be applied over
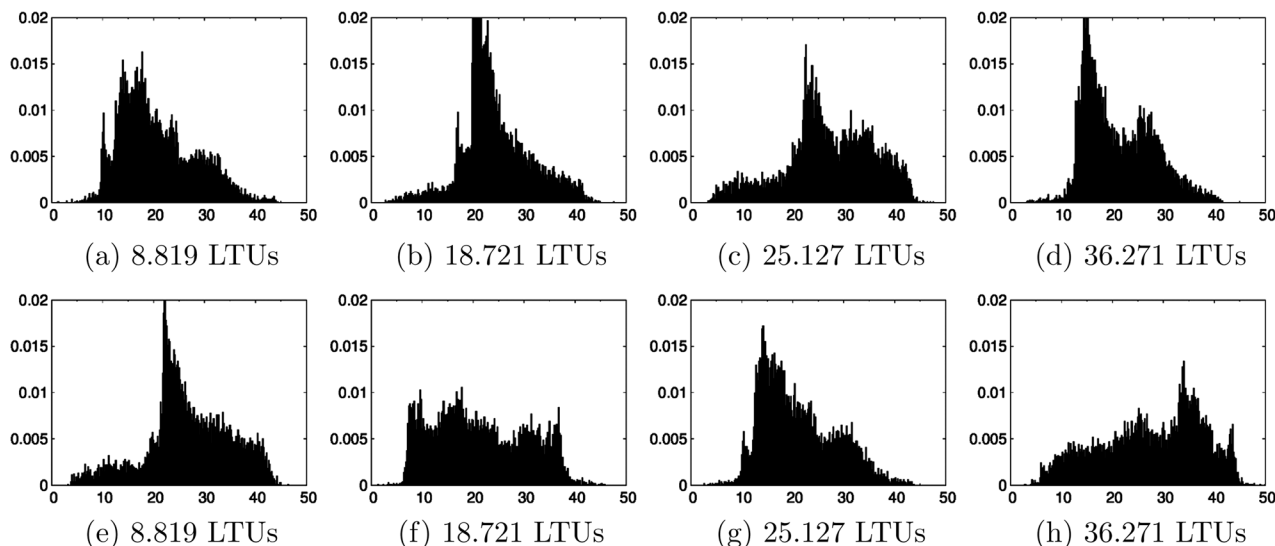

FIG. 14. Normalised frequency distributions for a 10 000 member IC ensemble at given time instants when (a)–(d) $f_i = 5$ and (e)–(f) $f_i = 5$ but the time series in ρ is inverted. The x-axis corresponds to the Z variable and y-axis as in Fig. 2. Some density in panels (b)–(e) extend beyond the scale.
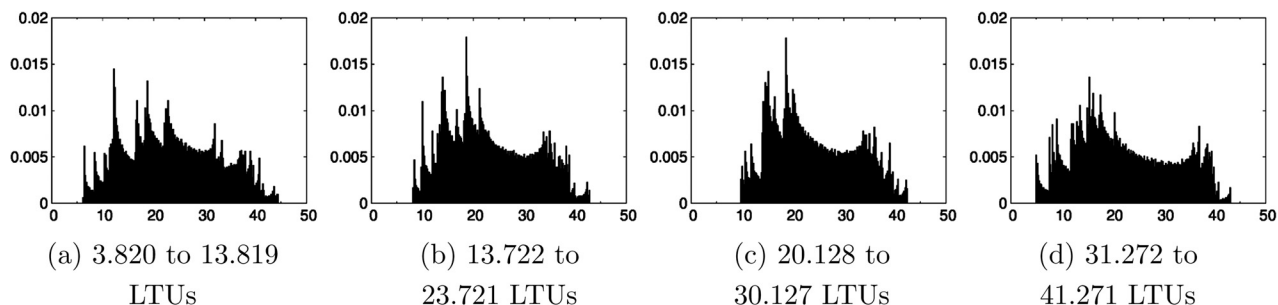
FIG. 15. Normalised frequency distributions for a single trajectory with ICs $(X_0, Y_0, Z_0) = (0.62, -0.98, 21.93)$, when $f_i = 5$ over 10 LTU intervals centred on: (a) $t = 8.819$ LTUs; (b) $t = 18.721$ LTUs; (c) $t = 25.127$ LTUs; (d) $t = 36.271$ LTUs. The x-axis corresponds to the Z variable and y-axis as in Fig. 2.

shorter periods? In the light of Fig. 14, one would expect not but this is such a commonly applied method in the analysis of climate and climate model timeseries[5,26,38,39] that it is worth, nevertheless, presenting results from such an approach in the nonperiodic L63 model.

In parallel with the analysis of climate timeseries, a single realisation is used to construct frequency distributions for time intervals centred on specific points in time. A single member of the ensemble, used to produce Fig. 14 with the non-inverted timeseries for ρ, is used and frequency distributions generated for 10 LTU time intervals centred on the time instants presented in Fig. 14. For example, the time interval centred on 8.819 LTUs (see Figs. 14(a) and 14(e)) includes all states from 3.820 to 13.819 LTUs.

The single trajectory distributions (Fig. 15) are substantially different to the corresponding IC ensemble climate distributions (Figs. 14(a)–14(d)) at an instant, indicating the failure of the kairodic assumption. If the time intervals were made gradually shorter, we would expect the single trajectory data to, at some point, begin to be drawn from a distribution which is approaching that of the IC ensemble, but reducing the number of data points will likely result in it still being a poor representation of the instantaneous climate.

E. Convergence of model ensembles for nonperiodic forcing in ρ

In Sec. III, the memory of the L63 model with regard to macro-IC uncertainty was investigated, and it was demonstrated that alternative IC ensemble distributions, originating near different parts of the attractor, converge towards a common distribution for fixed parameter conditions. It is not clear, however, whether IC ensembles originating in different regions of model state space will converge at all under periodic or non-periodic variations in ρ. Furthermore, if the ensembles do converge, how is the rate of convergence affected?

Memory of macro-ICs in the L63 model subject to non-periodic forcing is investigated with 10 000 member IC ensembles originating from the same four sets of ICs (Fig. 5) as used in the fixed parameter case but applying nonperiodic variations in ρ with frequency parameter $f_i = 5$. Rather than comparing the distributions to the standard stationary climate distributions, we compare them to the time varying ensemble distributions for $f_i = 5$ which were presented above and which were initialised from 10 000 ICs randomly distributed across the fixed $\rho = 28$ attractor. Fig. 16 shows the time variation of this comparison.

The first point to note is that all four ensembles converge to the same time varying distribution (Fig. 16). Macro-IC uncertainty does not in this case inhibit the long-term predictability of the model climate distributions when subject to nonperiodic fluctuations in ρ; the model and the "forcing" timeseries for ρ is sufficient to constrain the evolving distribution after some initial relaxation period. However, as observed for fixed parameters, the initial location of the IC ensemble dictates how rapidly the different ensembles converge; after 5 LTUs, the *IC 1* ensemble remains more dissimilar to the reference distributions than the other ensembles. It is also worth noting that the rate of convergence is faster than in the fixed parameter case; the ensembles converge after only 20 LTUs.
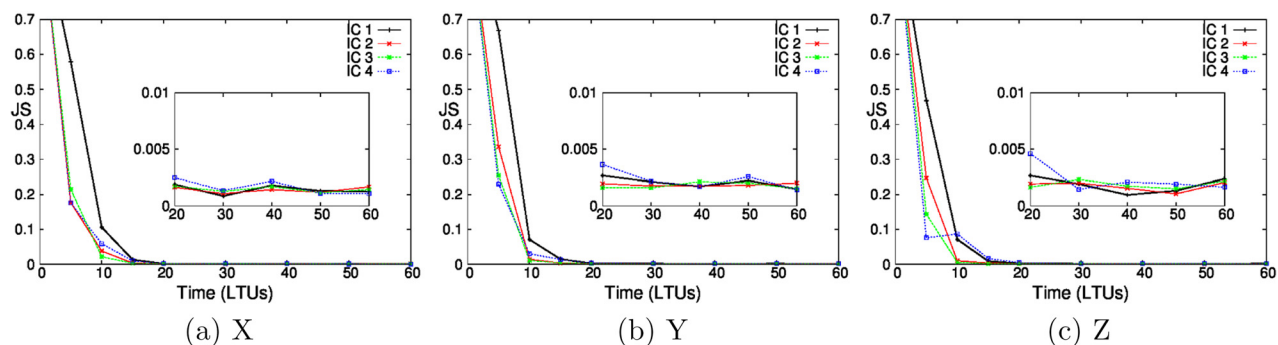

FIG. 16. JSD results showing the comparisons between IC ensemble distributions, from IC locations shown in Fig. 5 to the distributions resulting from an IC ensemble, with ICs extracted from the first 10 000 members of the standard climate distributions, at given time instants. In all model runs, ρ varies according to Eq. (10) with a wave frequency, $f_i = 5LTU^{-1}$.

These results may, however, be specific to the particular model setup studied here. Different nonlinear systems and possibly even oscillations involving different regions of the L63 phase space, macro-ICs, and periodic or non-periodic frequencies could potentially respond differently, possibly not converging at all.

VII. DISCUSSION

The output from experiments conducted on low-dimensional idealised models, such as the L63 model, are inevitably limited in their relevance to higher dimensional systems. One cannot expect the results described here to generalise in any specific way to higher-order climate models, let alone the real climate system. However, in exploring the rich dynamics of the L63 model, a better conceptual understanding of variability and change in complex nonlinear systems can be gained. This can help inform the way in which climate model experiments are designed and provides insight to guide the interpretation of the output from complex climate models.

In reality, there are multiple internal and external forcings with differing degrees of periodicity which exert an influence on the dynamic evolution of the climate system.[40–42] The cumulative effects of these individual components lead to aperiodic forcing time series. When the L63 model is subject to nonperiodic variations in ρ, as shown in Sec. VI, both resonance and path dependence are shown to be important factors in determining the climate model ensemble distributions. In guiding the design of climate model experiments to explore climatic uncertainties, this work suggests that it is important to assess the potential for resonance and hysteresis to alter the shape of climate variable distributions.

In Secs. II D and V B, it is shown that the kairodic assumption holds for fixed and periodic (sinusoidal) variations in ρ for sufficiently long model realisations. In the periodic case, however, either the ensemble distributions must represent a complete cycle or the single trajectory must only be sampled at the same point in the cycle as the ensemble. The parallel in climate modelling is that under stationary conditions, distributions over annual or diurnal cycles, or for points in those cycles, could be derivable from either single long simulations or from shorter ensembles.

However, in Sec. VI C, the kairodic assumption is shown to fail when the L63 model is subject to nonperiodic parameter variations. The parallel in climate science here relates to the wide range of different forcing variations experienced by the system on a range of timescales. The implication is that single realisations, or even small IC ensembles, of climate models may be unable to provide distributions which describe the model's climate at a point in time, or over the annual cycle or parts thereof (e.g., seasonal distributions); that is to say, distributions constructed over multiple years may substantially misrepresent those representative of a particular year.

These results have implications for the climate modelling community. Because of computational limitations, climate model simulations are rarely run with more than a handful of IC members.[33] When utilising climate model information to inform impact models (e.g., hydrological models), the kairodic assumption is therefore pervasive. If the behaviour exhibited in the L63 model was to be observed in more complex climate models, then the output of climate statistics based on single model realisations or small ensembles would be misleading for both model interpretation and as the basis for model derived predictions.

The memory of macro-IC uncertainty in the L63 model has also been explored. In the regions of parameter space explored here, convergence of IC ensembles is observed despite nonperiodic variations in the parameter ρ. Furthermore, the time period exhibiting memory of the IC location appears to be reduced in the case of parametric variations.

[1]E. N. Lorenz, "Deterministic nonperiodic flow," J. Atmos. Sci. **20**, 130–141 (1963).
[2]E. N. Lorenz, "Can chaos and intransitivity lead to interannual variability," Tellus **42A**, 378–389 (1990).
[3]J. D. Daron and D. A. Stainforth, "On predicting climate under climate change," Environ. Res. Lett. **8**(3), 034021 (2013).
[4]K. Fraedrich, "Estimating the dimensions of weather and climate attractors," J. Atmos. Sci. **43**, 419–432 (1986).
[5]IPCC, *Climate Change 2013: The Physical Science Basis. Contribution of Working Group I to the Fifth Assessment Report of the Intergovernmental Panel on Climate Change* (Cambridge University Press, Cambridge, United Kingdom and New York, NY, USA, 2013), Chap. Annex III: Glossary.
[6]D. A. Stainforth, M. R. Allen, E. R. Tredger, and L. A. Smith, "Confidence, uncertainty and decision-support relevance in climate predictions," Philos. Trans. R. Soc. A **365**, 2145–2161 (2007).
[7]M. Lakshmanan and S. Rajasekar, *Nonlinear Dynamics: Integrability, Chaos and Patterns* (Springer-Verlag, Berlin, Heidelberg, 2003), Chap. III, pp. 32–34.
[8]M. Chekroun, I. Zaliapin, and M. Ghil, "Pullback attractors in nonautonomous dynamical systems with delay: Applications to an enso model with seasonal forcing," *Geophysical Research Abstracts* (EGU General Assembly, 2010), Vol. 12.
[9]M. D. Chekroun, E. Simonnet, and M. Ghil, "Stochastic climate dynamics: random attractors and time-independent invariant measures," Physica D **240**(21), 1685–1700 (2011).
[10]M. D. McDonnell and D. Abbott, "What Is stochastic resonance? Definitions, misconceptions, debates, and its relevance to biology," Plos Comput. Biol. **5**(5), 1–9 (2009).
[11]H. W. Broer and G. Vegter, "Resonance and singularities," *Progress and Challenges in Dynamical Systems* (Springer Proceedings in Mathematics and Statistics, 2013).
[12]L. Gammaitoni, P. Hanggi, P. Jung, and F. Marchesoni, "Stochastic resonance," Rev. Mod. Phys. **70**(1), 223–287 (1998).
[13]R. Benzi, A. Sutera, and A. Vulpiani, "The mechanism of stochastic resonance," J. Phys. A **14**, L453 (1981).
[14]A. Crisanti, M. Falcioni, G. Paladin, and A. Vulpiani, "Stochastic resonance in deterministic chaotic systems," J. Phys. A **27**, L597–L603 (1994).

[15]A. Sutera, "Stochastic perturbation of a pure convectie motion," J. Atmos. Sci. **37**, 245–249 (1980).

[16]R. Benzi, G. Parisi, A. Sutera, and A. Vulpiani, "Stochastic resonance in climatic change," Tellus **34**, 10–16 (1982).

[17]S. M. Tobias and N. O. Weiss, "Resonant interations between solar activity and climate," J. Climate **13**, 3745–3759 (2000).

[18]R. Benzi, "Stochastic resonance: From climate to biology," Nonlin. Process. Geophys. **17**, 431–441 (2010).

[19]H. von Storch and F. W. Zwiers, *Statistical Analysis in Climate Research* (Cambridge University Press, Cambridge, UK/New York, 1999).

[20]J. C. Sprott, *Chaos and Time-Series Analysis* (Oxford University Press, 2003).

[21]D. Ruelle, "A measure associated with axiom-A attractors," Am. J. Math. **98**(3), 137–151 (1976); available at http://www.jstor.org/discover/10.2307/2373810?sid=21106318970383&uid=4&uid=2129&uid=2&uid=70&uid=3738032.

[22]J. P. Eckmann and D. Ruelle, "Ergodic theory of chaos and strange attractors," Rev. Mod. Phys. **57**(3), 617–656 (1985).

[23]S. H. Schneider, W. E. Easterling, and L. O. Mearns, "Adaptation: Sensitivity to natural variability, agent assumptions, and dynamic climate changes," Climatic Change **45**, 203–221 (2000).

[24]W. Burroughs, *Climate: Into the 21st Century* (Cambridge University Press: World Meteorological Organisation, 2003).

[25]M. New, M. Hulme, and P. Jones, "Representing twentieth-century space-time climate variability. Part I: Development of a 1961–90 mean monthly terrestrial climatology," J. Clim. **12**, 829–856 (1999).

[26]WMO, *Climatological Normals (CLINO) for the Period 1961–1990* (WMO/OMM, World Meteorological Organisation, Geneva, Switzerland, 1996), pp. 847, 768.

[27]J. Lin, "Divergence measures based on the Shannon entropy," IEEE Trans. Inf. Theory **37**(1), 145–151 (1991).

[28]M. Tabor, *Chaos and Integrability in Nonlinear Dynamics: An Introduction* (Wiley, New York, 1989), p. 206.

[29]T. N. Palmer, "Extended-range atmospheric prediction and the Lorenz model," Bull. Am. Meteorol. Soc. **74**, 49–65 (1993).

[30]S. Strogatz, *Nonlinear Dynamics and Chaos: With Applications to Physics, Biology, Chemistry and Engineering* (Perseus Books Group, 1994).

[31]See supplementary material at http://dx.doi.org/10.1063/1.4916789 for additional supporting figures.

[32]S. Kullback and R. A. Leibler, "On information and sufficiency," Ann. Math. Stat. **22**(1), 79–86 (1951).

[33]WCRP, *WCRP Coupled Model Intercomparison Project—Phase 5—CMIP5, CLIVAR Exchanges Special Issue* (World Climate Research Programme, 2011), Vol. 16.

[34]T. N. Palmer, "A nonlinear dynamical perspective on climate prediction," J. Clim. **12**, 575–591 (1999).

[35]D. J. Lea, M. R. Allen, and T. W. N. Haine, "Sensitivity analysis of the climate of a chaotic system," Tellus **52A**, 523–532 (2000).

[36]A. P. Rothmayer and D. W. Black, "Ensembles of the Lorenz attractor," Proc. Math. Phys. Sci. **441**(1912), 291–312 (1993).

[37]C. Sparrow, *The Lorenz Equations: Bifurcations, Chaos and Strange Attractors, Vol. 41 of Applied Mathematical Sciences* (Springer-Verlag, New York Inc., 1982).

[38]V. Lucarini, "Towards a definition of climate science," Int. J. Environ. Pollut. **18**(5), 413–422 (2002).

[39]D. B. Stephenson, M. Collins, J. C. Rougier, and R. E. Chandler, "Statistical problems in the probabilistic prediction of climate change," Environmetrics **23**(5), 364–372 (2012).

[40]J. R. Petit, J. Jouzel, D. Raynaud, N. I. Barkov, J.-M. Barnola, I. Basile, M. Bender, J. Chappellaz, M. Davis, G. Delaygue, M. Delmotte, V. M. Kotlyakov, M. Legrand, V. Y. Lipenkov, C. Lorius, L. Pepin, C. Ritz, E. Saltzman, and M. Stievenard, "Climate and atmospheric history of the past 420,000 years from the Vostok ice core, Antarctica," Nature **399**, 429–436 (1999).

[41]M. Ghil, "Natural climate variability," in *Encyclopedia of Global Environmental Change, Volume 1, The Earth System: Physical and Chemical Dimensions of Global Environmental Change* (John Wiley and Sons, Ltd., Chichester, 2002), pp. 544–549.

[42]D. Rind, "The Sun's role in climate variations," Science **296**, 673–678 (2002).